16TH EUROPEAN CONFERENCE ON EARTHQUAKE ENGINEERING THESSALONIKI 18 - 21 JUNE 2018

RESPONSE VALUES OF RECENT ACCELERATION RECORDS AND TIME HISTORY ANALYSIS OF ROCKING MOTION

Mizuo INUKAI[1], Tatsuya AZUHATA[2]

ABSTRACT

This paper describes the response values of acceleration records in recent years in the Section 2 and the time history analyses of rocking motion in the Section 3.
In the Section 2, the response values of acceleration records of 2016 Kumamoto Earthquake, Japan and 2015 Nepal Earthquake were analyzed. These response values were compared with those of the recent acceleration records.
When the period of analysis was less than 0.5 (sec), which were considered similar to the periods of low houses in wooden structures, steel structures or reinforced concrete structures, the maximum of inelastic response relative displacement was analyzed to be at most 23 (cm) of 2016 Kumamoto Earthquake. In this earthquake, a consecutive record of the Foreshock and the Main shock was also analyzed.
In the Section 3, the time history analyses of rocking motion were described. The rocking motion was usually discussed in dynamic soil-structure interaction (SSI). The equation of damped free motion of rocking for the rigid body was described in the equation of damped free motion of rocking. The relationship between the internal moment of the rigid body M and the angle θ was assumed with the positive rocking stiffness and the negative one. Because the stiffness (M/θ) was negative to be ($-mgh$), the complementary functions include the hyperbolic functions (sinh, cosh) and some constants. The similar response angle to the experimental results were when the damping factors at the angle zero were 0.3% or 0.7%.

Keywords: Response Values; Rocking Motion; Time History Analysis; Hyperbolic Function; Negative Stiffness; Imaginary Number

1. INTRODUCTION

This paper describes the response values of acceleration records in recent years in the Section 2 and the time history analyses of rocking motion in the Section 3.

2. RESPONSE VALUES OF ACCELERATION RECORDS IN RECENT EARTHQUAKES

This Section 2 describes the response values of acceleration records in of 2016 Kumamoto Earthquake, Japan and 2015 Nepal Earthquake.

2.1 Acceleration Records in Recent Years

Recent years, many earthquakes occurred and caused severe damage. In these earthquakes, many earthquake waves were recorded, for example, Kumamoto Earthquake, Japan in 2016 and Kathmandu of Nepal in 2015. These earthquake waves are very useful for the structural design of buildings. So, in this Section, the response values of recent acceleration records were analyzed to compare with the ones of earthquakes from 1940 to 2011 and artificial which were described in Inukai (2012).

[1]Chief Research Engineer, International Institute of Seismology and Earthquake Engineering (IISEE), Building Research Institute (BRI), Tsukuba City, Japan, inkm@kenken.go.jp
[2]Chief Research Engineer, IISEE, BRI, Tsukuba City, Japan, azuhata@kenken.go.jp

In Table 1, the earthquake waves were the main shock of 2016 Kumamoto Earthquake on 16 April 2016, [2004 Kawaguchi EW, Local Government] and [1995 Takatori NS, Japan Railroad].
In Table 2, the earthquake wave was 2015 Nepal Earthquake.

Table 1. Earthquake Waves for qCy* (= 0.2)

Earthquake Names [Earthquake Waves Names]	**Dire.**	**Peak Acc. (cm/sec^2)**	**Epi. Dist. (km)**	**Date and Time in Local Time**	**Remarks of Courtesy**
2016 Kumamoto Earthquake (Main shock)				16 April 2016.	
[20160416 Mashiki EW, L-Gov]	EW	825	6.4	01:25	L-Gov*1
[20160416 Mashiki EW2, KiK-net]	EW	1157	7.3		KiK-net,*2
[20160416 Nishihara EW, L-Gov]	EW	770	15.8		L-Gov*1
2016 Kumamoto Earthquake (Foreshock)				14 April 2016.	
[20160414 Mashiki EW, L-Gov]	EW	925	5.2	21:26	L-Gov*1
[20160414 Mashiki EW2, KiK-net]	EW	732	6.2		KiK-net,*2
[20160414 Nishihara EW, L-Gov]	EW*3	341	13.4		L-Gov*1
2004 Niigata-ken Chuetsu Earthquake				23 Oct. 2004. 17:56	
[2004 Kawaguchi EW, L-Gov]	EW	1676	2.8		L-Gov*4
1995 Kobe Earthquake				17 Jan. 1995.	
[1995 Takatori NS, JR]	NS	606	11.3	05:46	Japan Railroad

Notes) 1)qCy* : Design Shear Coefficient at Yielding Point referred to Section 2.2.
2)Dire. : Direction recorded the peak acceleration among the 2 horizontal directions of East and West or North and South.
3)Peak Acc. : Peak Acceleration
4)Epi. Dist. : Epicentral Distance
5)L-Gov*1 : Kumamoto Prefecture and Japan Meteorological Agency (JMA) in JMA(2016).
6)KiK-net*2 : Data of National Research Institute for Earth Science and Disaster Prevention in K-NET (2016).
7)EW*3 : In the Foreshock Wave [20160414 Nishihara EW, L-Gov], the direction for the analysis was EW as same as the other records in 2016 Kumamoto Earthquake while the maximum peak acceleration 532 (cm/sec^2) among the 2 horizontal directions of Nishihara Site was recorded in the direction of North and South.
8)L-Gov*4 : Niigata Prefecture and JMA in JMA (2004).

Table 2. Earthquake Wave for qCy (= 0.1)

Earthquake Names [Earthquake Waves Names]	**Dire.**	**Peak Acc. (cm/sec^2)**	**Epi. Dist. (km)**	**Date and Time in Local Time**	**Remarks of Courtesy**
2015 Nepal Earthquake				25 April 2015.	
[2015 KatNP NS, CESMD]	NS	160	59.9	11:56	CESMD*

Notes) 1)CESMD* : Center for Engineering Strong Motion Data in CESMD(2015).
2)Dire. : Direction same as Table 1
3)Peak Acc. : Peak Acceleration
4)Epi. Dist. : Epicentral Distance

2.2 Inelastic Dynamic Response Analysis Method

The response displacements of Single-Degree-of-Freedom (SDOF) can help us to understand how much displacement took place in storeys of structures during earthquake.
Fig. 1 shows the hysteresis property of Tri-linear Model for the inelastic dynamic analysis. In this analysis, Takeda Model of Takeda et al. (1970) was applied, which has the oriented point before the yielding point was the crack point in the opposite. The stiffness coefficient ${}_qk_4$ of unloading after the yielding point has some relationship with the stiffness ${}_qk_0$ between the yielding point and the crack point in the opposite side (${}_qk_4 = {}_qk_0(\delta y/\delta \text{peak})^{0.4}$). The other parameters of qCc, ${}_qk_1$, ${}_qk_2$ and ${}_qk_3$ were calculated by equations in Fig.1. Equations of qCc = 0.4・qCy and $({}_qk_2) = ({}_qk_1)/3$ were referred to Inukai et al. (2014). The period *T* for each SDOF analysis was calculated by the mass *m* and the secant stiffness *ky* in Equation 1. The value of damping coefficient *h* was 0.05

$$T = 2\pi\sqrt{\frac{m}{ky}} = \frac{2\pi}{\sqrt{{}_qk_y \cdot g}} = 2\pi\sqrt{\frac{\delta y}{qCy \cdot g}} \tag{1}$$

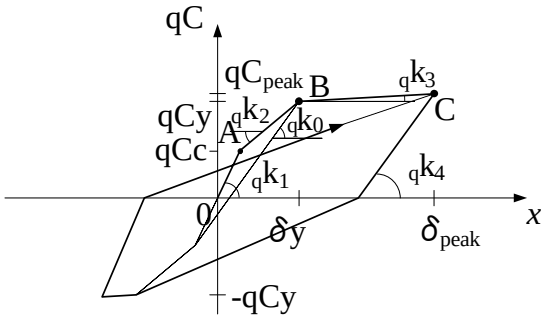

Notes)
(1) Takeda Model (The oriented point before yield point was the cracking point in the opposite side.)
(2) The stiffness coefficient ${}_qk_0$ was the slope of a line joining the yield point in one direction to the cracking point in the other direction.
(3) The stiffness coefficient ${}_qk_4$ of unloading after the yield point was defined by the slope ${}_qk_0$, δy and δpeak ; $${}_qk_4 = {}_qk_0\left(\frac{\delta y}{\delta \text{ peak}}\right)^{0.4}$$
(4) Other parameters were referred to Inukai et al. (2015).
(5) The shear coefficient of the cracking point qCc was 0.4 times of one of the yield point qCy ;. $$qCc = 0.4 \cdot qCy$$
(6) The initial stiffness coefficient ${}_qk_1$ was 2.2 times of the secant stiffness coefficient at the yield point ; $${}_qk_1 = 2.2 \cdot \frac{qCy}{\delta y}$$
(7) The second stiffness coefficient ${}_qk_2$ was one third of ${}_qk_1$; $${}_qk_2 = \frac{{}_qk_1}{3}$$
(8) The third stiffness coefficient ${}_qk_3$ was one thousandth of the secant stiffness coefficient at the yield point ; $${}_qk_3 = \frac{1}{1000}\frac{qCy}{\delta y}$$
(9) The secant stiffness coefficient at the yield point ${}_qk_y$ was the division of the secant stiffness by the weight ; $${}_qk_y = \frac{qCy}{\delta y} = \frac{ky}{mg}$$
(10) Shear Coefficient qC was the division of the storey shear force by the weight ; $$qC = \frac{\text{Storey Shear Force (Q)}}{\text{Weight } (m \cdot g)}$$
(11) qCy : Shear Coefficient at the yield point of A (qCy = 0.1, 0.2.)
(12) qC_{peak} : Shear Coefficient at the peak of B
(13) Q : Storey Shear Force (kN) ($= k \cdot x$)
(14) ${}_qk_0$, ${}_qk_1$, ${}_qk_2$, ${}_qk_3$, ${}_qk_4$: Stiffness Coefficient (1/cm) ; $${}_qk_i = \frac{\text{Initial Stiffness } k_i}{\text{Weight } (m \cdot g)}$$
(15) *h* : Damping factor (= 0.05)
(16) *g* : Gravity Acceleration (=980 (cm/sec^2))

Fig. 1 Hysteresis property of Tri-linear Model

2.3 Analysis Results

Analysis results are the response displacement spectra of 2016 Kumamoto Earthquake Main shock, Foreshock and other 10 records when Shear Coefficient qCy was 0.2. Other results are the one of 2015 Nepal Earthquake and other 10 records when Shear Coefficient qCy was 0.1.
The analyses were executed in the period from 0.1 (s) to 5.0 (s), and the spectra show the maximum values of the absolute values in each time history analysis.
The other 10 records, for qCy (=0.2), were 2011 Great East Japan Earthquake [2011 THU-1F N192E, BRI], [2011 Tsukidate NS, K-NET], [2011 Sendai NS, K-NET], [2011 Wakuya EW, JMA], 2007 Niigata-ken Chuetsu-Oki Earthquake [2007 Kashiwazaki NS, K-NET], 2004 Niigata-ken Chuetsu Earthquake [2004 Kawaguchi EW, L-Gov], [2004 Ojiya EW, K-NET], 1995 Kobe Earthquake [1995 Kobe NS, JMA], [1995 Takatori NS, JR] or BCJ Level2 <Artificial Earthquake Acceleration Data on Bedrock > [BCJ Level2 (Bedrock)].
According to Fig. 2 and Fig.3, when the period *T* was less than 0.5 (sec), to be considered similar to the periods of low houses in wooden structures, steel structures or reinforced concrete structures, the maximum of inelastic response relative displacement was analyzed to be at most 23 (cm) of [20160416 Mashiki EW, L-Gov] and the next one was [20160414 Mashiki EW, L-Gov], [20160416 Mashiki EW2, KiK-net], [20160416 Nishihara EW, L-Gov], [20160414 Mashiki EW2, KiK-net] or [20160414 Nishihara EW, L-Gov], respectively. These response displacements of 2016 Kumamoto

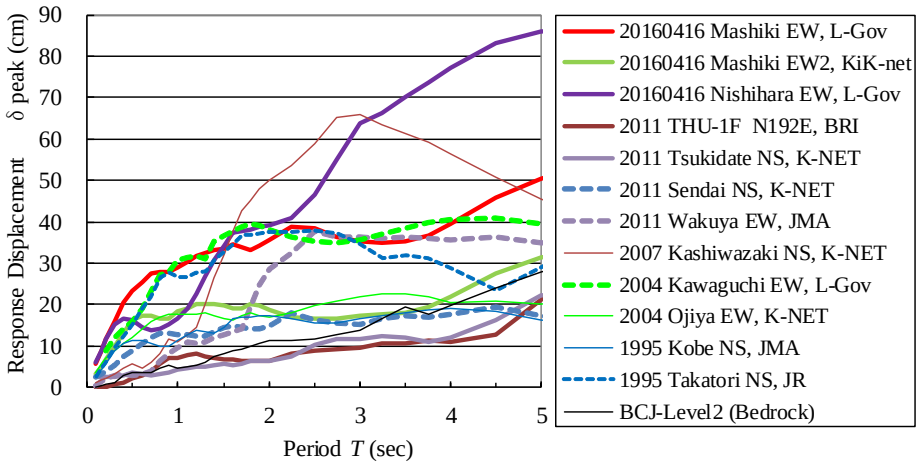

Fig. 2 Inelastic Response Displacement Spectra of 2016 Kumamoto Earthquake Main shock and other records (qCy=0.2, *h* =0.05)

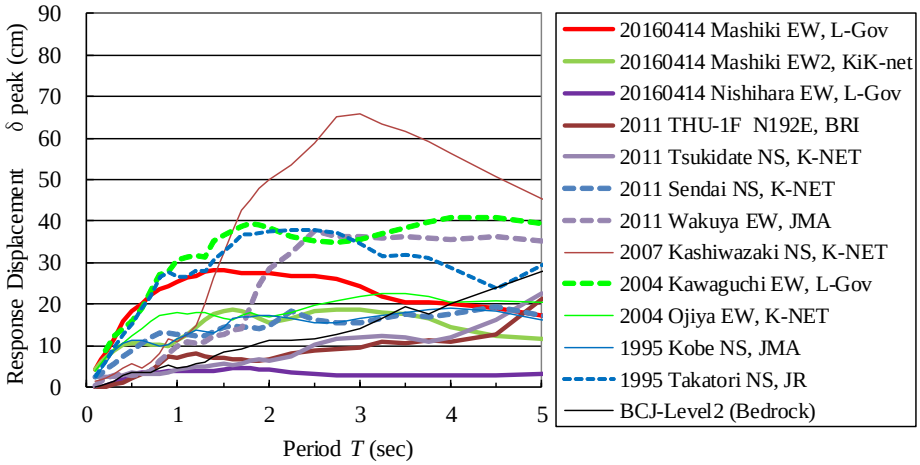

Fig. 3 Inelastic Response Displacement Spectra of 2016 Kumamoto Earthquake Foreshock and other records (qCy=0.2, *h* =0.05)

Earthquake Main shock or Foreshock near the epicenter were equal or greater than ones of 2004 Kawaguchi EW or 1995 Takatori NS.
When the period was larger than 5 (sec), the response displacement of the Main shock in [Mashiki, L-Gov], [Mashiki, KiK-net] or [Nishihara, L-Gov] was still increasing and the same increasing was also analyzed in [2015 KatNP NS, CESMD] (Inukai, Azuhata, Morita, et al. (2017)).
The earthquake waves were affected by the ground condition and the structures around the measuring points. On the soft soil condition, the response displacement was considered to be larger in the range of long period.
In 2016 Kumamoto Earthquake, there were the Foreshock on 14th Apr. 2016 and the Main shock on 16th Apr. 2016, 2 days later. Therefore, the consecutive records of them were also analyzed. The record length of Mashiki Town, L-Gov. and Nishihara Village, L-Gov. were 120.00 (sec) and the one of Mashiki, KiK-net was 300.00 (sec). The consecutive record length of them were 240.00 and 600.00 (sec) respectively. These consecutive records names show “20160414+16” in Fig. 4.
According to the Fig. 4, the response displacement of [20160414+16 Mashiki EW, L-Gov] were greater than one of [20160416 Mashiki EW, L-Gov] or [20160414 Mashiki EW, L-Gov]. The one of [20160416 Mashiki EW2, KiK-net] were also greater than one of [20160416 Mashiki EW2, KiK-net] or [20160414 Mashiki EW2, KiK-net] from the period 0.1 (sec) to 4 (sec).
On the other hand, the response displacement of [20160414+16 Nishihara EW, L-Gov] were smaller than one of [20160416 Nishihara EW, L-Gov] when the period was less than 1.0(sec).

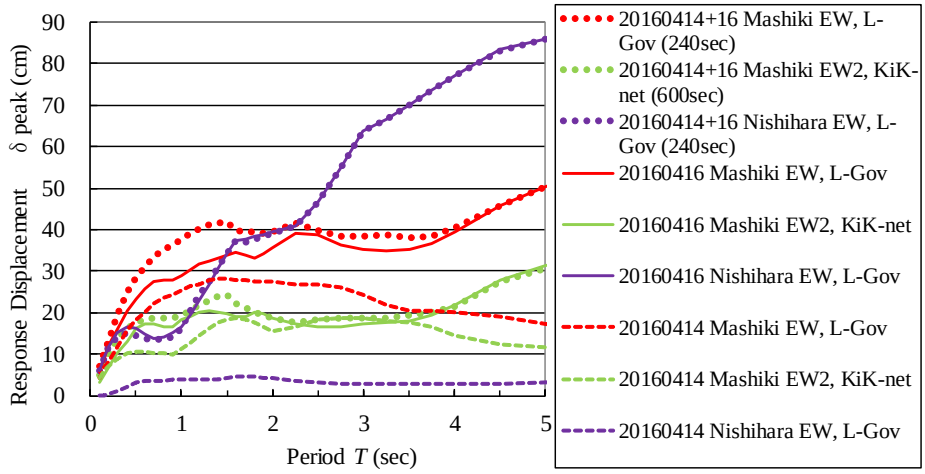

Fig. 4 Inelastic Response Displacement Spectra of 2016 Kumamoto Earthquake Main shock and Foreshock, 2016 Main shock or 2016 Foreshock (qCy=0.2, h =0.05)

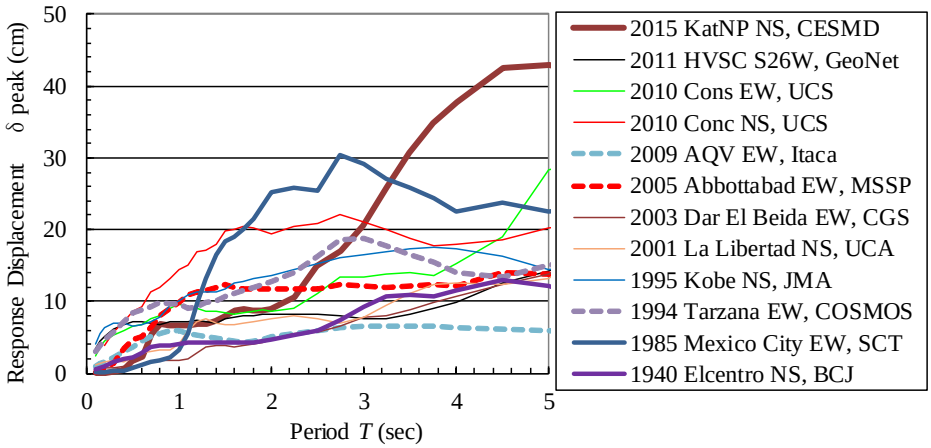

Fig. 5 Inelastic Response Displacement Spectra of 2015 Nepal Earthquake and other records (qCy=0.1, h =0.05)

In these analyses, after the response values of the Foreshock were calculated at the start displacement zero (cm), the ones of the Main shock were calculated consecutively at the residual displacement after the Foreshock. That means why the response displacement of the consecutive records were different from the ones of the Main shock, some ones were greater and some others were smaller.
The other 10 records, for qCy (=0.1), were 2011 New Zealand Christchurch Earthquake [2011 HVSC S26W, GeoNet], 2010 Chile Earthquake [2010 Cons EW, UCS], [2010 Conc NS, UCS], 2009 Italy L'Aquila Earthquake [2009 AQV EW, Itaca], 2005 Pakistan Earthquake [2005 Abbottabad EW, MSSP], 2003 Algeria Earthquake [2003 Dar El Beida EW, CGS], 2001 El Salvador Earthquake [2001 La Libertad NS, UCA], [1995 Kobe NS, JMA], 1994 Northridge Earthquake [1994 Tarzana EW, COSMOS], 1985 Michoacan Mexico Earthquake [1985 Mexico City EW, SCT] or [BCJ Level2 (Bedrock)].
According to Fig. 5, when the period T was about 3.5 (sec), the maximum of inelastic response relative displacement was analyzed to be a maximum of [2015 KathNP NS, CESMD]. This value was still increasing to more than 3 (m) when the period was more than 3.5 (sec).

3. TIME HISTORY ANALYSES OF ROCKING MOTION

This Section 3 describes non-linear time history response analysis for rocking and the comparison between the analyses and the test results.

3.1 Non-Linear Time History Response Analysis for Rocking

Generally, the equation of damped free motion of rocking in Fig. 6 was described in Equation 2. In Fig. 6, m was the mass, B(=2b) was the width of the rigid body, H (=2h) was the height and g was the gravity acceleration. In Equation 2, according to Inukai et al. (2015), I was the moment of inertia at the ground surface ($I = m h^2$), c_I was the damping coefficient, k_I was the rocking stiffness, $\ddot{\theta}$ was the response acceleration of angle, $\dot{\theta}$ was the response velocity of angle, h_I was the length of the moment arm by external forces and θ was the angle. M (=$k_I\theta$) was the internal moment of the rigid body, the relationship between M and θ was shown in Fig. 6 (b) (Ishiyama (1980)). When k_I was assumed to be too large at θ=0 and M was assumed to be 0, mgb or $-mgb$, the mathematical solutions for each θ are very difficult.

$$I\ddot{\theta} + c_I\dot{\theta} + k_I\theta = -m\ddot{y}h_I \tag{2}$$

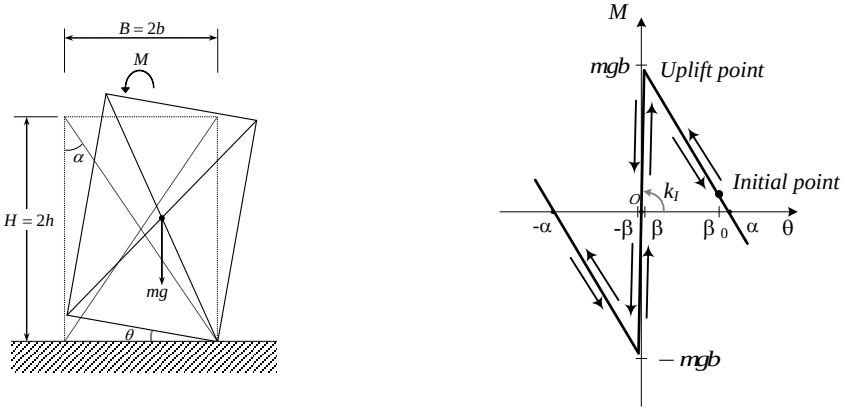

(a) Rigid Body in Motion (b) Relationship of M and θ

The ground was rigid. α was the angle of the width to the height (b/h).

Fig. 6 Rigid Body in Motion and the Relationship between the internal moment M of the centre of the gravity and the rotation angle of rocking θ when the ground was rigid

If the start of analysis has some horizontal displacement without velocity, and during the motion there were no external forces, the analysis should be simple (Inukai, Azuhata (2017)). Therefore, in Fig. 6(b), in this non-linear time history response analysis for rocking, the relationship of $M - \theta$ was assumed, the rocking stiffness of the ground k_I (>0) was also assumed when θ was around zero from $-\beta$ to β and M was decreased to be zero after M was almost mgb until θ was almost α. The initial point was when θ was some value and the velocity was zero.
The relationship of $M - \theta$ and the equation of damped free motion of rocking were as follows;

$$\beta < \theta \quad : \quad M = mgh\,(\alpha - \theta) \tag{3}$$
$$-\beta \le \theta \le \beta \quad : \quad M = k_I\,\theta \tag{4}$$
$$\theta < -\beta \quad : \quad M = -mgh\,(\alpha + \theta) \tag{5}$$
$$I\ddot{\theta} + c_I\dot{\theta} + M = 0 \tag{6}$$

In order to make analysis for rocking, a stiffness at θ (= 0) was needed. If the start of analysis has some horizontal displacement without velocity, and if during the motion there were no external forces, the analysis should be simple.
These complementary functions at time t were known. Normally, to solve Equation 6 for Equation 4, the solution $\theta = C\,e^{pt}$ should be considered. To solve Equation 3, after the characteristic equations using p doesn't have the constant α, the solution $\theta - \alpha \equiv \theta_{\alpha} = C\,e^{pt}$ should be considered. Thus, the response velocity $\dot{\theta}_{\alpha} = \mathrm{d}(\theta_{\alpha})/\mathrm{d}t = \mathrm{d}(\theta\text{-}\alpha)/\mathrm{d}t = \mathrm{d}\theta/\mathrm{d}t = \dot{\theta}$ and the response acceleration $\ddot{\theta}_{\alpha} = \mathrm{d}^2(\theta_{\alpha})/\mathrm{d}t = \mathrm{d}^2(\theta\text{-}\alpha)/\mathrm{d}^2t = \mathrm{d}^2\theta/\mathrm{d}^2t = \ddot{\theta}$ were not dependent on α. Equation 3 has the negative stiffness. Therefore, these characteristic equations using p were as follows;

$$p^2 + 2h_1\omega_1 p - \omega_1^2 = 0 \tag{7}$$
$$p^2 + 2h_0\omega_0\, p + \omega_0^2 = 0 \tag{8}$$

Damping factor h_0, h_1 and circular frequency ω_0, ω_1 were real numbers.
The solutions p_1, p_2 of Equation 7 were

$$p_1 = -h_1\omega_1 + \omega_1\sqrt{h_1^2 + 1} \tag{9}$$
$$p_2 = -h_1\omega_1 - \omega_1\sqrt{h_1^2 + 1} \tag{10}$$

In Equation 9 and 10, $h_1\omega_1$ was always smaller than $\omega_1\sqrt{h_1^2 + 1}$, ($h_1\omega_1 < \omega_1\sqrt{h_1^2 + 1}$). Therefore, always p_2 was negative and p_1 was positive ($p_2 < 0 < p_1$). Because p_1 was positive, the complementary function $\theta = C_1 e^{p_1 t} + C_2 e^{p_2 t}$ were described in Equation 11, 12 and 13 using hyperbolic functions (sinh, cosh) and constant α or trigonometric functions (sin, cos).

$$\beta < \theta \quad : \quad \theta = \alpha + \mathrm{e}^{-h_1\omega_1 t}(A_1\cosh\omega_{n1}t + B_1\sinh\omega_{n1}t) \tag{11}$$
$$-\beta \le \theta \le \beta \quad : \quad \theta = \mathrm{e}^{-h_0\omega_0 t}(A_0\cos\omega_{n0}\,t + B_0\sin\omega_{n0}\,t) \tag{12}$$
$$\theta < -\beta \quad : \quad \theta = -\alpha + \mathrm{e}^{-h_2\omega_2 t}(A_2\cosh\omega_{n2}t + B_2\sinh\omega_{n2}t) \tag{13}$$

The undetermined coefficients, A_1, B_1 and others, were calculated from the initial values and the stiffness respectively (Muto et al. (1960)). The functions of velocity and acceleration were defined as the differential equations at time t of the above functions of displacement.
All parameters, h_0, h_1, ω_0, ω_1, ω_{n0}, ω_{n1} and others, were real numbers. Finally, the results of Equation 11, 12 and 13 give the real numbers.
When θ was close to β, after the initial point, the interval time in the analysis was 0.0005 (sec) (=2,000Hz) in Equation 7. After the time, when θ was β, was defined, the initial values of θ and the

velocity $\dot{\theta}$ in Equation 8 were defined to continue the analysis.
These analyses were executed to be compared with the test results of the following section.
By the way, on the above analyses, it was described that all parameters were real numbers, it was because the 2 characteristic equations of Equation 9 and 10 were used respectively for the negative stiffness or the positive stiffness according to the values of θ. But it should be understood that the negative stiffness was used in the analyses. So, in the following section, the damping factor h_1 for the negative stiffness was described to be imaginary number using imaginary unit i (= $\sqrt{-1}$). This imaginary number h_1 was calculated by the negative stiffness k_1 (= $-mgh$), the imaginary number ω_1 (= square root of (k_1/I) ($\omega_1 = \sqrt{k_1/I} = \sqrt{-(mgh/I)} = i\sqrt{mgh/I} = i\sqrt{g/h}$)), the damping coefficient c_I which was a constant real number ($h_1\ \omega_1 = c_I/(2I) = h_0\ \omega_0 = h_2\ \omega_2$) and h_1 was equal to $c_I/(2I\ \omega_1)$, ($h_1 = c_I/(2I\ \omega_1)$).

3.2 Rocking Specimen

In recent years, the experimental project of free standing concrete column specimens by placing some situations of ground was produced, when the damped free motion given an initial value of the horizontal displacement was performed by the several corporations (Takenaka Corp. et al. (2013)). Specimens, height 3.7m, width 1.1m, the thickness 1.5m and the weight 104.9 kN in the free end. The

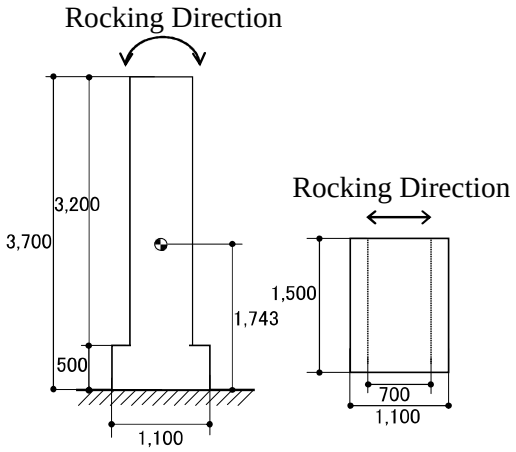

(a) Elevation (b) Plan
Fig.7 Rocking Specimen (Reinforced concrete column on concrete slab)

(a) Rocking Specimen under loading (b) Photo of Rocking Specimen under loading
Fig. 8 Rocking Specimen under loading (Reinforced concrete column on concrete slab)

height of the centre of mass (◓) was 1.743m. The specimens were placed on the ground, were inclined to the top displacement horizontally 0.375m and so on.
After the horizontal tension force was released, the rocking damped free motions were conducted (Fig. 7 and Fig. 8). The release points for one loading were at the top displacement horizontally 0.125m for 2 times, 0.250m for 2 times, 0.375m for 2 times and 0.125m for 1 time. The total number of loadings was 7 times. In the experiment, the acceleration and the displacement of some parts were measured, when these data were compared to this analysis of the horizontal force and the horizontal displacement of the centre of mass.

3.3 Analysis and Results

In the analysis, while the damping ratio was a parameter, the response moment M and the response angle θ of the centre of mass were calculated and compared with the experimental values. In Fig. 9, The Idealized relationship between M and θ shows the typical points which were the $M=mgb=$ 57.7kN·m was in y-axis and the angle of the width to the height (b/h) (=550/1,743=0.316 rad.) in x-axis. In experimental relationship, the Uplift point (M,θ) = (50kN·m, 0.0005rad.) and the Initial point (37kN·m, 0.113rad.) were proposed. The Initial point was located under the line of the Idealized relationship. These points were exchanged to the relationship between the shear coefficient (F/mg), which was shear force (F) divided by the weight (mg), and the horizontal displacement (x) of the centre of mass. For the idealized and experimental F/mg and x, the idealized point was (F/mg, x) = (0.316-, 0.0cm) or the proposed points were the Uplift point (F/mg, x) = (0.273-, 0.09cm) and the Initial point (0.202-, 19.7cm).

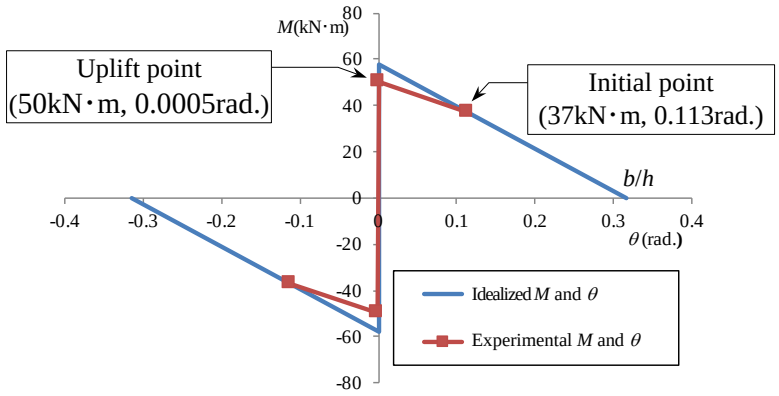

Fig. 9 Relationship of M and θ of the centre of mass

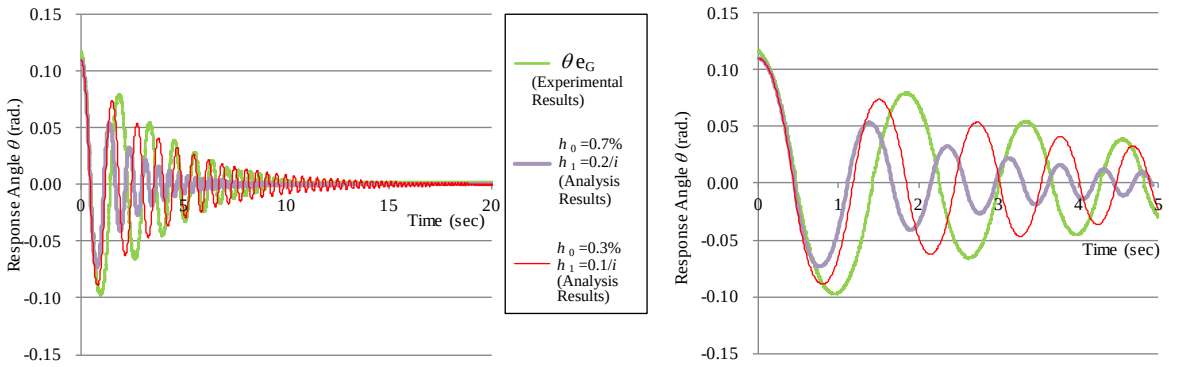

Notes are same as the Notes of Fig. 10 (a)

(a) Until 20 (sec) (b) Until 5 (sec)

Fig. 10 Comparison of Experimental Result (δe_G) and Analysis Results (h_0=0.3% and h_0=0.7%)

According to the elastic stiffness, k_I in Equation 4 or ω_0 in Equation 12, the period of the contact of the specimen to the ground was calculated to be 0.11 second. Outside of the elastic, the response functions include the hyperbolic functions (sinh, cosh) without trigonometric functions in Equation 11 and 13 and don't have any period.

As the results, Fig. 10 shows the non-linear time history response analysis results of the damped free motion of the Rocking Specimen. In Fig. 10, θ e_G was the response angle of the centre of gravity and started at 0.113rad. when the top displacement horizontally was 0.375 m in the first time among the 2 times loadings. Until 10 (sec), θ e_G has some amplitude and after 10 (sec), it has some residual angle.

According to the relationship of Fig. 9 and Equations 11 – 13, the analysis results of θ were also shown in Fig. 10. They were 2 results when h_0 was 0.3% and h_1 was 0.1/i or h_0 was 0.7% and h_1 was 0.2/i. When h_0 was 0.3%, the amplitudes of θ were close to the experimental data until 10 (sec). When h_0 was 0.7%, the amplitudes of θ were close to the experimental data after 10 (sec). Fig.10 (b) shows the same results of until 5 (sec) of 20 (sec) in Fig. 10 (a), while the interval times between the peaks were not similar in the experimental data and the 2 results. In the analysis, the grounding times of the specimen were calculated to be about 0.002 (sec) or more.

4. CONCLUSIONS

In this paper, the response values of acceleration records in recent years, the time history analyses of rocking motion were described. The main points of these results were as follows;

(1) The response displacements of 2016 Kumamoto Earthquake Main shock or Foreshock near the epicenter were equal or greater than ones of 2004 Niigata-ken Chuetsu Earthquake, 1995 Kobe Earthquake or others.
(2) When the period was larger than 5 (sec), the response displacement of 2016 Kumamoto Earthquake Main shock near the epicenter were still increasing and the same increasing was also analyzed in 2015 Nepal Earthquake.
(3) When the stiffness in rocking motion was negative, the response horizontal force and the response horizontal displacement were calculated by the hyperbolic functions.
(4) The period by the stiffness during the contact of the rocking specimen to the ground in this analysis was considered to be 0.11 (sec).
(5) The similar response displacements of the rocking motion to the experimental results were when the damping factors at the displacement zero were 0.3% or 0.7%.
(6) The grounding times of the rocking specimen in this analysis were calculated to be about 0.002 second or more.
(7) The comparison between the analysis and the experimental results of the rocking motion were not so much similar, therefore, the coupled system like Soil-Structure Interaction should be necessary.

5. REFERENCES

Center for Engineering Strong Motion Data Homepage (2015). Lamjung, Nepal Earthquake of 25 April, http://www.strongmotioncenter.org/cgi-bin/CESMD/selectpage.pl?Lamjung_us20002926%2FNPKATNP=on&Raw=on

Inukai M (2012). Response Values of Earthquake Waves and Structural Assessment of Cultural Heritage, *Proceeding of the 15th World Conference on Earthquake Engineering, International Association for Earthquake Engineering*, Lisbon, Portugal, Sept., Paper ID.: 2012-2336.

Inukai M, Azuhata T (2017). Damped Free Motion of Rocking Specimens in Non-Linear Time History Response Analysis, *Proceedings of the VII International Conference on Coupled Problems in Science and Engineering*, International Center for Numerical Methods in Engineering (CIMNE), Ebook, pp.227-233, Rhodes Island, Greece.

Inukai M, Azuhata T, Morita K, et al. (2017). Out-of-plane Dynamic Test of Unreinforced Masonry Walls Retrofitted andResponse Values of Recent Acceleration Records, *Proceeding of the 16th World Conference on*

Earthquake Engineering, International Association for Earthquake Engineering, Santiago Chile, Jan., Paper ID.: 2017-75.

Inukai M, Kashima T, Saito T (2014). Response Values in Hysteresis Properties by Acceleration Records, *Usb of 2ECEES (The Second European Conference on Earthquake Engineering and Seismology)*, No. 227, Istanbul, Turkey.

Inukai M, Kashima T, Saito T, Azuhata T (2015). Predominant Periods of Multi-Degree-of-Freedom System Analysis and Dynamic Soil-Structure Interaction for Building Structures, *Proceedings of the VI International Conference on Coupled Problems in Science and Engineering*, International Center for Numerical Methods in Engineering (CIMNE), Ebook, pp.278-289, Venice, Italy.

Ishiyama Y (1980). Review and Discussion on Overturning of Bodies by Earthquake Motions, *BRI Research Paper* No. 85, Building Research Institute, Ministry of Construction, June, Tsukuba, Japan.

Japan Meteorological Agency (JMA) Homepage (2016). Strong Motion Data of Kumamoto Earthquake on 01:25, 16 April, Local Government and JMA,
http://www.data.jma.go.jp/svd/eqev/data/kyoshin/jishin/1604160125_kumamoto/index2.html (in Japanese).

JMA Homepage (2004). Strong Motion Data of Niigata-ken Chuetsu Earthquake on 17:56, 23 Oct., Local Government and JMA, http://www.data.jma.go.jp/svd/eqev/data/kyoshin/jishin/041023_niigata/nigata_main.htm (in Japanese).

Kyoshin Network K-NET Homepage (2016). http://www.kyoshin.bosai.go.jp/kyoshin/quake/index_en.html, National Research Institute for Earth Science and Disaster Resilience, Japan.

Muto, K. Umemura, H. and Sonobe, Y (1960). Study of the Overturning Vibration of Slender Structures. *Proceeding of the Second World Conference on Earthquake Engineering*, Science Council of Japan and the Committee for the Second World Conference on Earthquake Engineering, vol.2, pp.1239-1261, Association for Science Documents Information, Tokyo, Japan.

Takeda T, Sozen M.A, et al. (1970). Reinforced Concrete Response to Simulated Earthquakes, *Journal of the Structural Division, Proceedings of the ASCE*, Vol. 96, No.ST12, December, pp.2557-2573.

Takenaka Corporation and Taisei Corporation (2013). Study of Structural Design Methods of Buildings Considering Uplift Behavior, *Summary of Report for 2013 Review and Promotion Project of Building Codes*, Housing Bureau, Ministry of Land, Infrastructure, Transport and Tourism, Tokyo, Japan.
http://www.mlit.go.jp/common/001037167.pdf (in Japanese)